

THE UNIVERSITY OF MANITOBA

AN INVESTIGATION OF COAXIAL YAGI LOOP ARRAYS

by

Alireza Shoamanesh

A THESIS

SUBMITTED TO THE FACULTY OF GRADUATE STUDIES

IN PARTIAL FULFILLMENT OF THE REQUIREMENTS FOR THE DEGREE

OF MASTER OF SCIENCE

DEPARTMENT OF ELECTRICAL ENGINEERING

WINNIPEG, MANITOBA

October 1975

**"AN INVESTIGATION OF COAXIAL  
YAGI LOOP ARRAYS"**

by

**ALIREZA SHOAMANESH**

**A dissertation submitted to the Faculty of Graduate Studies of  
the University of Manitoba in partial fulfillment of the requirements  
of the degree of**

**MASTER OF SCIENCE**

**© 1975**

**Permission has been granted to the LIBRARY OF THE UNIVER-  
SITY OF MANITOBA to lend or sell copies of this dissertation, to  
the NATIONAL LIBRARY OF CANADA to microfilm this  
dissertation and to lend or sell copies of the film, and UNIVERSITY  
MICROFILMS to publish an abstract of this dissertation.**

**The author reserves other publication rights, and neither the  
dissertation nor extensive extracts from it may be printed or other-  
wise reproduced without the author's written permission.**

*To my parents*



## ABSTRACT

The electrical characteristics of coaxial circular loop arrays are investigated by a numerical solution of the integral equation for the loop currents. Loop currents are expressed in a Fourier series of the azimuthal coordinate and the resonant property of the loop antenna is utilized to improve the convergence of the series. For arrays with different loop sizes this resonant effect is beneficially used to reduce their electrical length. As a result, with a negligible loss in the accuracy of the computation, the required labour for the investigation of the array characteristics is reduced significantly.

The effect of array parameters on its characteristics such as the input admittance, the directive gain and the radiation pattern are then studied. For a specific wire cross section extensive design data for arrays of three to twelve elements are computed.

## ACKNOWLEDGEMENTS

The author wishes to thank Dr. L. Shafai for his continuous interest, helpful advice, cheerful and able guidance in all phases of this work.

I would also like to thank my friends and colleagues for their discussions and suggestions, and in particular, Mr. Rashid Ali Rafek for reading the manuscript, and Mrs. Darlene Lowry for typing it.

The financial assistances provided by the National Research Council of Canada (Grant A-7702) and the Department of Electrical Engineering of the University of Manitoba are greatly appreciated.

Alireza Shoamanesh

## TABLE OF CONTENTS

CHAPTER		PAGE
	ABSTRACT . . . . .	(i)
	ACKNOWLEDGEMENTS . . . . .	(ii)
	TABLE OF CONTENTS . . . . .	(iii)
	LIST OF FIGURES . . . . .	(v)
	LIST OF TABLES . . . . .	(viii)
	LIST OF MOST USED SYMBOLS . . . . .	(x)
I	INTRODUCTION . . . . .	1
II	FORMULATION OF THE PROBLEM . . . . .	9
	2.1 Introduction . . . . .	9
	2.2 Formulation of the Problem . . . . .	9
	2.3 Evaluation of $K_{ij}^n$ . . . . .	14
	2.4 Discussions on $K_{ij}^n$ . . . . .	18
	2.5 Current Distribution and the Admittance. . . . .	20
	2.6 The Radiation Field and the Directive Gain . . . . .	23
III	RESONANCE EFFECTS IN ARRAY OF CIRCULAR LOOP ANTENNA . . . . .	26
	3.1 Introduction . . . . .	26
	3.2 Resonance Effects . . . . .	26
	3.3 Application to Input Admittance . . . . .	42
	3.4 Computation of Dominant Modes . . . . .	47
	3.5 Typical Pattern Calculation . . . . .	50
IV	INVESTIGATIONS OF THE FAR FIELD PATTERN OF THE LOOP ARRAY . . . . .	57
	4.1 Introduction . . . . .	57
	4.2 Radiation Pattern of the Loop Arrays . . . . .	57
	4.3 Effect of Reflector Spacing . . . . .	60
	4.4 Effect of the Reflector Size . . . . .	63
	4.5 Effect of Director Spacings . . . . .	66

CHAPTER		PAGE
	4.6 Effects of the Director Size . . . . .	70
	4.7 Effects of the Exciter Size . . . . .	76
	4.8 Effects of wire cross section . . . . .	79
	4.9 Summary . . . . .	82
V	DESIGN DATA FOR SHORT AND MEDIUM LENGTH LOOP YAGI ARRAYS . . . . .	83
	5.1 Introduction . . . . .	83
	5.2 Treatment of the Problem . . . . .	83
	5.3 Optimum Adjustment of the Feeder- Reflector Combination . . . . .	84
	5.4 Outline of Results . . . . .	87
VI	CONCLUSIONS . . . . .	101
	REFERENCES . . . . .	103
	APPENDIX A Convergence of Equation (2.20) . . . . .	106
	APPENDIX B Comparison Between $Z_{ij}^n$ and $Z_{ii}^n$ . . . . .	115

## LIST OF FIGURES

FIGURE		PAGE
2.1	Geometry of the array . . . . .	10
2.2	Determination of three regions where $\alpha = 4 \sin^2 \frac{\delta}{2} \gg \left(\frac{a_i}{b_i}\right)^2$ and $\delta \ll 1$ . . . . .	15
3.1	Dominant mode of each array element at $\phi=0^\circ$	30
3.2	Current distributions on the active element	31
3.3	Radiation pattern of a "12-element" loop array . . . . .	32
3.4	Current distributions on the active element	35
3.5	Radiation pattern of a "12-element" loop array in the H-plane . . . . .	36
3.6	Dominant mode of each array element at $\phi=0^\circ$	38
3.7	Radiation pattern of a "12-element" array in the H-plane . . . . .	39
3.8	Dominant mode of each array element at $\phi=0^\circ$	40
3.9	Dominant mode of each array element at $\phi=0^\circ$	41
3.10	A "12-element" loop array divided into two groups . . . . .	50
3.11	Radiation pattern of a "12-element" loop array in the H-plane . . . . .	53
3.12	Radiation pattern of a "12-element" loop array in the H-plane . . . . .	54
3.13	Radiation pattern of a "12-element" loop array in the H-plane . . . . .	55
3.14	Radiation pattern of a "12-element" loop array in the H-plane . . . . .	56
4.1	Radiation patterns in the H-plane for different reflector spacings . . . . .	61



FIGURE		PAGE
4.2	Behaviour of the directive gains, $G_r$ and $G_d$ , and the input admittance for different reflector spacing . . . . .	62
4.3	Radiation patterns in the H-plane for various reflector sizes . . . . .	64
4.4	Behaviour of the directive gains, $G_r$ and $G_d$ , and the input admittance for different reflector sizes . . . . .	65
4.5	Radiation patterns in the H-plane for various director spacings . . . . .	67
4.6	Radiation patterns in the H-plane for various director spacings . . . . .	68
4.7	Behaviour of the directive gains, $G_r$ and $G_d$ , and the input admittance for various director spacing . . . . .	69
4.8	Radiation patterns in the H-plane for different director size . . . . .	71
4.9	Radiation patterns in the H-plane for different director size . . . . .	72
4.10	Radiation patterns in the H-plane for different director size . . . . .	73
4.11	Effects of the director size on the directive gains, $G_d$ and $G_r$ , and the input admittance . . . . .	74
4.12	Effects of the director size on the directive gains, $G_d$ and $G_r$ , and the input admittance . . . . .	75
4.13	Radiation patterns in the H-plane for various exciter sizes . . . . .	77
4.14	Effects of the exciter size on the directive gains and the input admittance . . . . .	78
4.15	Radiation patterns in the H-plane for different wire cross section . . . . .	80
4.16	Effects of wire cross section in the directive gains, $G_r$ and $G_d$ , and the input admittance . . . . .	81

FIGURE		PAGE
5.1	The conductance and the susceptance of a circular loop of radius $b$ . . . . .	85
5.2	Directive gain of feeder-reflector combination in the positive $z$ direction as a function of reflector size for various reflector spacing . . . . .	86
5.3	Maximum directive gain of feeder-reflector combination in the positive $z$ direction as a function of reflector spacing . . . . .	86
A.1	Examples of computed values of $a_n^m$ . . . . .	110
A.2	Examples of computed values of $a_n^m$ . . . . .	111
A.3	Approximation $\sum_{m=0}^M a_n^m$ of $\text{Re}(K_{ij}^n)/kb_i$ and its error $a_n^{M+1}/(1-r)$ . . . . .	112
A.4	Examples of computed values of $a_n^m$ . . . . .	113
A.5	Approximation $\sum_{m=0}^M a_n^m$ of $\text{Re}(K_{ij}^n)/kb_i$ and its error $a_n^{M+1}/(1-r)$ . . . . .	114
B.1	Comparison between the imaginary parts of generalized self and mutual impedance . . . . .	117
B.2	Comparison between the imaginary parts of generalized self and mutual impedance . . . . .	118

LIST OF TABLES

TABLE		PAGE
2.1	Approximate equations for $K_{ii}^n$ . . . . .	16
2.2	Approximate equations for $K_{ii}^n$ . . . . .	17
3.1	The current modes on each loop of a "12-element" loop array . . . . .	29
3.2	The current modes on each loop of a "12-element" loop array . . . . .	34
3.3	Comparison of the exact and approximate results for $y_{22}^n$ . . . . .	44
3.4	Comparison of the exact and approximate values of the input admittance . . . . .	46
5.1	Computed characteristics of "three-element" circular loop Yagi arrays . . . . .	91
5.2	Computed characteristics of "four-element" circular loop Yagi arrays . . . . .	92
5.3	Computed characteristics of "five-element" circular loop Yagi arrays . . . . .	93
5.4	Computed characteristics of "six-element" circular loop Yagi arrays . . . . .	94
5.5	Computed characteristics of "seven-element" circular loop Yagi arrays . . . . .	95
5.6	Computed characteristics of "eight-element" circular loop Yagi arrays . . . . .	96
5.7	Computed characteristics of "nine-element" circular loop Yagi arrays . . . . .	97
5.8	Computed characteristics of "ten-element" circular loop Yagi arrays . . . . .	98
5.9	Computed characteristics of "eleven-element" circular loop Yagi arrays . . . . .	99

TABLE		PAGE
5.10	Computed characteristics of "twelve-element" circular loop Yagi arrays . . . . .	100
A.1	Required values of $M$ for satisfactory convergence . . . . .	109
B.1	Required values of $m_o$ after which $Z_{ij}^n$ can be assumed diagonal . . . . .	116

## LIST OF MOST USED SYMBOLS

$a_i$	radius of wire cross section of the ith-element
$b_i$	radius of the ith-lement in a circular loop array ...
$C_{gi}$	gap capacitance
$d_D$	director spacing
$d_{ij}$	the separation distance between the ith and the jth element
$d_r$	reflector spacing
$E_\theta$	$\theta$ component of the electric field
$E_\phi$	$\phi$ component of the electric field
$E_{2n}$	Weber Lommel function of order 2n
$G_d$	directive gain in the positive z direction
$G_r$	directive gain in the negative z direction
$H_0^2$	zero-order Hankel function of the second kind
$h_{n+2m}^2$	second kind spherical Hankel function of order n+2m
$J_{2n}$	Bessel function of the first kind of order 2n
$I_i(\phi_i)$	total current
$I_j^n$	coefficient of the nth current mode
$k$	wave number in free space
$K_{ij}^n$	nth coefficient of Fourier series
$R_{ij}$	distance between two current components normalized by radius $b_i$
$U_i(\theta_i)$	a function equal to unity at the driving point and zero elsewhere
$V_i$	driving voltage of the ith element
$W_{ij}(\phi_i - \phi_j)$	kernel of integral

$n$	
$Z_{ij}$	generalized self and mutual impedance
$Y_{ij}^n$	generalized self and mutual admittance
$Y_2$	input admittance of loop Yagi array
$\gamma$	Euler's constant
$\delta\phi_i$	gap width of the driving point of the ith-element
$\epsilon_0$	permittivity of free space
$\eta_0$	intrinsic impedance of free space
$\eta_{n+2m}$	(n+2m)th order spherical Bessel function of the 2nd kind
$\mu_0$	permeability of free space
$\lambda$	wave length in free space
$\Omega_i$	thickness parameter of the ith-element
$\omega$	angular frequency

## CHAPTER I

### INTRODUCTION

A circular loop antenna, like a dipole, is one of the most common structures and has been the subject of many theoretical studies. Historically, small loop antennas were used as direction finders and flux detectors. As a radiator, the radiation pattern of a small loop antenna shows a figure of eight shape in the vertical plane involving the loop axis. As its size increases in terms of wavelength, the radiation in the axial direction increases and becomes maximum when the circumference is about one wavelength long [1]-[2]. As a result, a highly directive beam in the axial direction may be obtained by an array of coaxial loops of proper dimension.

A coaxial loop array with only one active element is the most common configuration. Its operating principle is similar to that of a Yagi-Uda array, but for a 2-element array a gain difference of about 1.8 dB in favor of the loop array is reported [3]. Unfortunately, published data for loop arrays of more than 2 elements is scarce. It is however reported that the radiation characteristics of loop arrays above the ground plane are less affected by the electrical properties of the soil, when compared with those of dipole arrays [4]. In addition, the use of parasitic loop arrays in place of dipoles has resulted in the elimination of corona problems at high altitudes [3]. These beneficial properties of loop arrays justify further investigation of their characteristics.

There are no difficulties in evaluating the radiation characteristics of a loop which is small with respect to the wavelength of operation. Here a uniform current distribution is assumed, and expressions for the radiated field are easily formulated [5]. For a larger loop, a more realistic current distribution must be found. G. Glinski has assumed a hyperbolic cosine form for the current distribution, similar to that of a lossy parallel-wire transmission line, in order to explain the experimental results for the horizontal radiation pattern of a comparatively large loop. To simplify his analysis, he has retained only the first few terms of an infinite series of the field expressions. This approximation, however, restricts his formula to loops in which the circumference is less than one-half a wavelength [6].

Several other methods have also been applied in the past to the analysis of a thin loop antenna in free space. One of the methods is the electromotive force method, or simply emf, for the determination of antenna impedance, where a current distribution corresponding to that of a wire of zero thickness is assumed. In general, the current distribution on an extremely thin wire antenna can be assumed to approximate a sine wave form very closely. Because of this the self impedance, determined by applying the emf method to an assumed sine wave current distribution, is generally a good practical approximation. Thus, a calculation of the antenna impedance by the emf, gives results, which are quite close to the actual values, except in the region around anti-resonance [7].



Another method which involves a more precise and practical theory, requires the computation of the current distribution from which the impedance is then determined. This technique requires the solution of integral equations by various approximation methods, of which the successive approximation method [1]-[2] and the series expansion method [ 8 ]-[11] are representative.

The first general analysis of a circular loop as a transmitting antenna appears to have been carried out by Hallen [ 8 ]. He analyzed circular loop antennas driven by an idealized delta function generator and obtained a solution, again in the form of a Fourier series, for the current and impedance. However, owing to the occurrence of a singularity or a very large value in the Fourier coefficient, when the index  $n$  is close to a certain large number determined by the loop's geometry, Hallen limited its application to loop antennas small compared to the wavelength. He explained that this nonconvergent series might be the result of his assumption of the one-dimensional flow of the current. Moreover, the individual terms were complicated and their evaluation and summation involved a somewhat difficult numerical task.

After Hallen's theory, Storer avoided the contribution from the large term by first replacing the Fourier series by a corresponding integral and then evaluating the integral using the Cauchy principle value. He provided extensive tables and graphs of the impedance, admittance and current distribution

for loops up to a wavelength in circumference and a number of different wire sizes [9]. Storer also examined the validity of the constant current distribution on a small loop and was led to the conclusion that loops larger than  $kb = 0.2$  ( $k = \frac{2\pi}{\lambda}$ ) can not be considered small.

T.T. Wu re-examined the problem of evaluating the Fourier series. He pointed out that assuming that the current flows along the center of the conductor, as with Hallen and Storer it does not converge everywhere on the antenna [10]. He explained that the satisfactory values obtained under this assumption were due to a false approximation. He examined the surface current distribution on a perfectly conducting loop and verified that the obtained Fourier series for  $I(\phi)$  converges everywhere except at the driving point ( $\phi=0$ ).

Later, King et al. [12] computed the input admittance of a circular loop by taking a partial summation of the infinite series obtained by Wu. They suggested that a Fourier series solution with 20 terms is satisfactory for determining the admittance of thin ( $\Omega = 2 \ln \frac{2\pi b}{a} \geq 10$ ) and small ( $kb \leq 2.5$ ) loops in air and dissipative media. Here  $k$ ,  $a$ , and  $b$  are the free space propagation constant and the wire and loop radii, respectively.

Inagaki et al. by assuming a finite gap at the driving-point gave a theoretical basis for determining the required number of terms in current and admittance computations [11]. They obtained an expression for the driving-point admittance in which the gap capacitance is a lumped representation of the

effect of the gap width. According to their analysis, the driving-point admittance can be treated apart from the gap capacitance, independent of the gap width. It thus is calculated by a partial summation of the Fourier series truncated at a term whose order is equal to the ratio of the loop radius to conductor radius.

On the other hand, Iizuka et al. [13] have analyzed two identical parallel loop antennas. They have decomposed the voltage and current into symmetric and antisymmetric components. As a result, the simultaneous integral equations for the distribution of current along the loops have been converted into a single integral equation similar to that for an isolated circular loop antenna which has already been studied. This method, however, is not applicable to antennas with loops of different circumference.

More recently the properties of an array of coaxial circular loop antennas with arbitrary circumferences have been analyzed by means of Fourier series expansions, with emphasis on the existence of finite gaps at the driving-points [14]. The expressions for the current distribution on each loop and the input admittance involve matrix inversion, where the dimension of the matrix is related to the array size. Thus, in investigations of loop arrays the required computer time and storage increase with the array size and for very large arrays become excessive.

This thesis considers coaxial loop arrays and utilizes the resonant property of loops to develop an efficient method for investigation of their characteristics. The current distri-

bution on each loop is expressed by Fourier series around the resonant mode and the Fourier coefficients are found numerically from the integral equation satisfied by the currents. It is shown that for resonant loops a single mode adequately describes the current distribution and a rapid calculation of the antenna parameters is generally feasible. For loops of arbitrary size, other modes are however significant, but a selection of a few modes adjacent to the nearest resonant modes usually provides an accurate representation. Such an approximation further simplifies the problem, if the array consists of loops of different sizes. Here, the resonant modes of loops are different and a given mode may not have a significant excitation in certain loops. As a result, the non-resonant loops can usually be neglected, which effectively reduces the electrical length of the array for such modes. This phenomenon further reduces the computation time and is used whenever possible. Chapter III is devoted to the investigation of these properties.

Chapter IV considers the effects of array parameters on the input admittance, the radiation field and the directivity of the loop yagi array. It will be seen that the effects of altering the reflector spacing and size are negligible in the forward direction whereas the input impedance of the array and its directive gain  $G_r$  in the negative  $z$  direction are very much dependent on these alterations. As a result, the reflector size or spacing may be used to vary the back lobe level and the impedance of the array. The driven loop dimensions and the wire cross section have negligible effect on the forward

radiation, but again have considerable effect on the array's input impedance.

It is also shown in Chapter IV that there are two principle ways by which the far field pattern of a Yagi loop array may be controlled. One is to vary the director spacing while holding the element circumference and reflector spacing constant. The second is to vary the director size while holding all other parameters fixed. Either one of these two ways will have a considerable effect on the far-field patterns. Numerical results show that when the exciter size is about a wave length, the director sizes must be less than or equal to the wave length, otherwise the far field patterns will not be useful.

The importance of loop Yagi arrays has already been discussed in [3] and [15]. Unfortunately, there exists very little information on design data for these type of arrays. The prime intention of Chapter V is to present numerical data for rapid design of uniform loop Yagi arrays in which the combination of the exciter and reflector is optimum for the directive gain in the forward direction. The data are for arrays containing between 3 to 12 elements when the director size,  $kb$ , changes from 1 to 0.7 with  $\Delta(kb) = 0.1$ , and the director spacing,  $d_D$ , alters from  $0.1\lambda$  to  $0.3\lambda$  with  $\Delta(d_D) = 0.05\lambda$ . From these tables it is seen that for the director circumference  $kb = 0.9$  the directive gain  $G_d$  has the largest value for any director spacing as long as the array contains more than two directors. The maximum value of directive gain  $G_d$  is found

to be 15.2 db, which is for the particular array of 10 directors at a spacing of  $0.3\lambda$ .

## CHAPTER II

### FORMULATION OF THE PROBLEM

#### 2.1 Introduction

An array of circular loops composed of  $N$  elements with arbitrary circumferences, arranged parallel in a row is analyzed for the case of a finite gap at the driving-point. Integral equations for the current distributions are obtained by expressing the electric field, through the use of Helmholtz integrals, in terms of currents and equating the total electric field to zero along the wire surface. A solution for the integral equations is sought with the aid of Fourier-series expansions of the kernels and the currents. Then the integral equations are reduced to a set of linear simultaneous equations for the Fourier coefficients of the electric currents of the same order. A solution of this set gives the unknown coefficients which are then used to evaluate the required antenna characteristics. In particular, it is shown that the self admittance may be obtained as a sum of two parts: a finite series truncated at a number determined by the ratio of the circular loop to the wire cross section radii and a gap capacitance. The mutual admittance, on the other hand, can be obtained from a finite series only.

#### 2.2 Formulation of the Problem

Consider an array consisting of  $N$  circular loops of arbitrary circumferences and arranged parallel to each other with their centers on the  $z$  axis, figure (2.1). The radius

of the  $i$ th loop, the radius of the conductive wire, and the driving-point voltage are denoted by  $b_i$ ,  $a_i$ , and  $V_i$ , respectively.

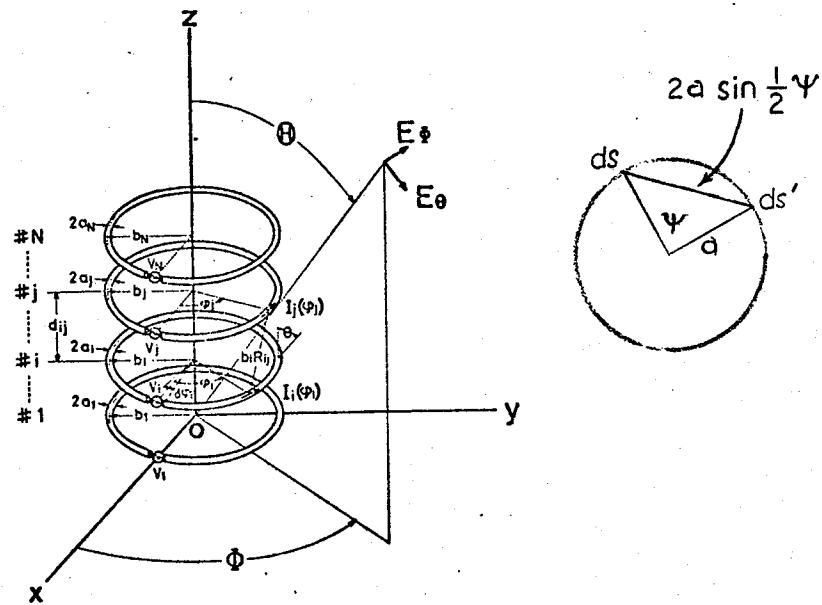


Figure 2.1 Geometry of the array.

It is assumed that

$$\frac{b_i}{a_i} \gg 1 \quad \text{and} \quad \frac{a_i}{\lambda} \ll 1 \quad (2.1)$$

where  $\lambda$  is the wave length of the signal in free space.

The array is immersed in an infinite isotropic homogeneous medium, where its complex propagation constant is



$k = \beta - j\alpha$ . If the medium is air  $\alpha = 0$  and  $\beta = \omega \sqrt{\epsilon_0 \mu_0} = 2\pi/\lambda = k$ , where  $\epsilon_0$  and  $\mu_0$  are the permittivity and the permeability of the air, respectively. This thesis considers the latter case only, when the array is located in the air.

It is assumed that the driving-point gap width  $b_i \delta\phi_i$  is finite and that the current  $I_i(\phi_i)$  on the  $i$ th element flows uniformly in the  $\psi$  direction along the conductor surface. Following the procedure in [8]-[10] for a single loop, the integral equation satisfying the boundary conditions of the electric field on the surfaces of  $N$  circular loops may be shown to be [14]

$$-\frac{V_i}{b_i \delta\phi_i} U_i(\phi_i) = j \frac{\eta_0}{4\pi b_i} \sum_{j=1}^N \int_0^{2\pi} [k b_j \cos(\phi_i - \phi'_j) + \frac{1}{k b_i} \frac{\partial^2}{\partial \phi_i^2} W_{ij}(\phi_i - \phi'_j) I_j(\phi'_j) d\phi'_j] \quad (2.2)$$

where  $i = 1, 2, 3, \dots, N$  and

$$W_{ij}(\phi) = \begin{cases} \frac{1}{2\pi} \int_0^{2\pi} \frac{\exp[-jkb_i R_{ii}(\phi, \psi)]}{R_{ii}(\phi, \psi)} d\psi, & i=j \\ \frac{\exp[-jkb_i R_{ij}(\phi)]}{R_{ij}(\phi)}, & i \neq j \end{cases} \quad (2.3)$$

$$(2.4)$$

where  $I_i(\phi_i)$  is the current on the  $i$ th loop,  $k = \frac{2\pi}{\lambda}$  is the propagation constant, and  $\eta_0 = \sqrt{\frac{\mu}{\epsilon}} = 120\Omega$  is the characteristic impedance of free space.  $U_i(\phi_i)$  is equal to 1 within the driving-point gap and is zero elsewhere. The distance  $R_{ij}$  between two currents, normalized by the loop radius  $b_i$  and for  $i = j$  is

$$R_{ii}(\phi, \psi) = [4 \sin^2 \frac{\phi}{2} + 4 \left(\frac{a_i}{b_i}\right)^2 \sin^2 \frac{\psi}{2}]^{\frac{1}{2}} \quad (2.5)$$

and when  $i \neq j$  and assuming  $d_{ij} \gg a_i$ , it is

$$\begin{aligned} R_{ij}(\phi) &= [4 \left(\frac{b_j}{b_i}\right)^2 \sin^2 \frac{\phi}{2} + \left(\frac{d_{ij}}{b_i}\right)^2 + \left(\frac{b_j}{b_i} - 1\right)^2]^{\frac{1}{2}} \\ &= [1 + \left(\frac{b_j}{b_i}\right)^2 + \left(\frac{d_{ij}}{b_i}\right)^2 - 2 \left(\frac{b_j}{b_i}\right) \cos \phi]^{\frac{1}{2}} \end{aligned} \quad (2.6)$$

The contribution of the magnetic current existing at the driving point is omitted in the right hand side of equation (2.2) but will later be introduced as an adjustment for the gap capacitance.

In order to solve the above simultaneous integral equations the current  $I_j(\phi_i)$  and the kernel  $W_{ij}(\phi)$  are expanded into Fourier series

$$I_j(\phi_j) = \sum_{n=0}^{\infty} I_j^n \cos n \phi_j \quad (j=1, 2, \dots, N) \quad (2.7)$$

$$W_{ij}(\phi) = \sum_{n=-\infty}^{\infty} K_{ij}^n e^{-jn\phi} \quad (i, j=1, 2, \dots, N) \quad (2.8)$$

where

$$K_{ij}^n = K_{ij}^{-n} = \frac{1}{2\pi} \int_0^{2\pi} K_{ij}^n(\psi) d\psi \quad (2.9)$$

where for  $i = j$

$$K_{ii}^n(\psi) = K_{ii}^{-n}(\psi) = \frac{1}{2\pi} \int_0^{2\pi} \frac{e^{-jkb_i R_{ii}(\phi, \psi)}}{R_{ii}(\phi, \psi)} \cdot e^{jn\phi} d\phi \quad (2.10)$$

and for  $i \neq j$

$$K_{ij}^n = K_{ij}^{-n} = \frac{1}{2\pi} \int_0^{2\pi} \frac{e^{-jkb_i R_{ij}(\phi)}}{R_{ij}(\phi)} e^{jn\phi} d\phi \quad (2.11)$$

An introduction of equations (2.7) and (2.8) into the right hand side of equation (2.2), after some manipulation gives [14]

$$\beta_i^n = \frac{\sin n \left(\frac{\delta\phi_i}{2}\right)}{n \frac{\delta\phi_i}{2}} V_i = \sum_{j=1}^N Z_{ij}^n I_j \quad (2.12)$$

$$(i = 1, 2, \dots, N, \quad n \geq 0)$$

where

$$Z_{ij}^n = \begin{cases} 1 & , \quad n = 0 \\ \frac{j\pi\eta_0}{2} (kb_j \frac{K_{ij}^{n+1} + K_{ij}^{n-1}}{2} - \frac{n^2}{kb_i} K_{ij}^n) & , \quad n \geq 1 \end{cases} \quad (2.13)$$

Equation (2.12) in the matrix form is

$$(Z_{ij}^n) (I_j) = (\beta_i^n) \quad , \quad n > 0 \quad (2.14)$$